Direct Detection of Calmodulin Tuning by Ryanodine Receptor Channel Targets Using a Ca^{2+}-Sensitive Acrylodan-Labeled Calmodulin†

Bradley R. Fruen, Edward M. Balog, Janet Schafer, Florentin R. Nitu, David D. Thomas, and Razvan L. Cornea*

Department of Biochemistry, Molecular Biology and Biophysics, University of Minnesota, Minneapolis, Minnesota 55455

Received August 13, 2004; Revised Manuscript Received October 15, 2004

ABSTRACT: Calmodulin (CaM) activates the skeletal muscle ryanodine receptor (RyR1) at nanomolar Ca^{2+} concentrations but inhibits it at micromolar Ca^{2+} concentrations, indicating that binding of Ca^{2+} to CaM may provide a molecular switch for modulating RyR1 channel activity. To directly examine the Ca^{2+} sensitivity of RyR1-complexed CaM, we used an environment-sensitive acrylodan adduct of CaM. The resulting ^{ACR}CaM probe displayed high-affinity binding to, and Ca^{2+}-dependent regulation of, RyR1 similar to that of unlabeled wild-type (WT) CaM. Upon addition of Ca^{2+}, ^{ACR}CaM exhibited a substantial (>50%) decrease in fluorescence ($K_{Ca} = 2.7 \pm 0.8$ μM). A peptide derived from the RyR1 CaM binding domain ($RyR1_{3614-43}$) caused an even more pronounced Ca^{2+}-dependent fluorescence decrease, and a ≥10-fold leftward shift in its K_{Ca} (0.2 ± 0.1 μM). In the presence of intact RyR1 channels in SR vesicles, ^{ACR}CaM fluorescence spectra were distinct from those in the presence of $RyR1_{3614-43}$, although a Ca^{2+}-dependent decrease in fluorescence was still observed. The K_{Ca} for ^{ACR}CaM fluorescence in the presence of SR (0.8 ± 0.4 μM) was greater than in the presence of $RyR1_{3614-43}$ but was consistent with functional determinations showing the conversion of ^{ACR}CaM from channel activator (apoCaM) to inhibitor (Ca^{2+}CaM) at Ca^{2+} concentrations between 0.3 and 1 μM. These results indicate that binding to RyR1 targets evokes significant changes in the CaM structure and Ca^{2+} sensitivity (i.e., CaM tuning). However, changes resulting from binding of CaM to the full-length, tetrameric channels are clearly distinct from changes caused by the RyR1-derived peptide. We suggest that the Ca^{2+} sensitivity of CaM when in complex with full-length channels may be tuned to respond to physiologically relevant changes in Ca^{2+}.

Calmodulin (CaM)[1] is a ubiquitous, highly conserved intracellular Ca^{2+} sensor, capable of binding and regulating diverse intracellular targets. Crystal and NMR structures of CaM in complex with different peptide targets have revealed multiple and distinct mechanisms of target binding (*1*, *2*). These structural data illustrate how binding to a particular target dictates the three-dimensional (3D) structure of CaM. In this way, target binding also determines CaM's sensitivity to Ca^{2+} such that a particular complex may respond to changing Ca^{2+} concentrations within a range appropriate for the regulation of a particular cellular process. Accordingly, pronounced and specific "tuning" of CaM Ca^{2+} affinities has been observed in the presence of soluble peptide fragments derived from various targets (*3*−*5*).

The type 1 ryanodine receptor (RyR1) is the major CaM binding protein in sarcoplasmic reticulum (SR) membranes isolated from skeletal muscle (*6*−*8*). Each tetrameric RyR1 channel binds four CaMs with high affinity (*9*, *10*), and 3D reconstructions based on cryoelectron microscopy show CaM bound within a crevice of the channel's cytoplasmic assembly (*11*). Binding of CaM to RyR1 channels promotes a leftward shift in the biphasic Ca^{2+} dependence of channel activity. This shift is explained by the opposing effects of apoCaM, which activates the channel in <1 μM Ca^{2+}, and Ca^{2+}CaM, which inhibits the channel in >1 μM Ca^{2+} (*12*).

Hamilton and co-workers have identified a critical region for CaM binding within the RyR1 primary sequence (*10*), and demonstrated that a peptide derived from this region ($RyR1_{3614-43}$) displays a high affinity for both apoCaM and Ca^{2+}CaM (*13*). More recently, a second noncontiguous region within RyR1 has also been implicated in CaM binding (*14*), and current models suggest that the CaM binding pocket is formed by neighboring subunits of tetrameric RyR1. Measurements of the intrinsic tryptophan fluorescence of the $RyR1_{3614-43}$ peptide in complex with CaM (*15*) have indicated that this peptide target promotes a substantial increase in CaM's affinity for Ca^{2+} ($K_d = 58$ nM), suggesting that formation of the inhibitory Ca^{2+}CaM species requires only nanomolar Ca^{2+} concentrations. In contrast, functional

† This work was supported by American Heart Association Grant 0265225Z (to R.L.C.) and National Institutes of Health Grants AR050144 (to B.R.F.) and GM031382 (to D.D.T.).

* To whom correspondence should be addressed. Phone: (612) 626-2660. Fax: (612) 624-5121. E-mail: corne002@umn.edu.

[1] Abbreviations: acrylodan, 6-acryloyl-2-dimethylaminonaphthalene; ^{ACR}CaM, acrylodan adduct of T26C-CaM; $^{ACR}CaM_{1234}$, acrylodan adduct of T26C-CaM_{1234}; apoCaM, Ca^{2+}-free CaM; BSA, bovine serum albumin; Ca^{2+}CaM, Ca^{2+}-bound CaM; CaM, calmodulin; CaM_{1234}, CaM mutant with reduced Ca^{2+} sensitivity due to glutamate to alanine substitutions within each of CaM's four EF-hands; DTT, dithiothreitol; GSH, reduced glutathione; GuHCl, guanidine hydrochloride; K_D, dissociation constant; MALDI-TOF MS, matrix-assisted laser desorption ionization time-of-flight mass spectroscopy; PIPES, 1,4-piperazinediethanesulfonic acid; RyR, ryanodine receptor; $RyR1_{3614-43}$, synthetic peptide replicating the RyR1 sequence spanning residues 3614−3643; SDS−PAGE, sodium dodecyl sulfate−polyacrylamide gel electrophoresis; SR, sarcoplasmic reticulum; T26C-CaM, CaM mutant with a threonine to cysteine mutation at residue 26; WT, wild-type.

10.1021/bi048246u CCC: $30.25
Published on Web 12/10/2004

studies demonstrate that much higher Ca^{2+} concentrations ($\sim$1 μM) are required for inhibition of full-length RyR1 channels (*9*, *12*, *16*). Thus, the particular structure and Ca^{2+} sensitivity of CaM when in complex with RyR1 remain undefined, although this information is key to resolving the potential roles of CaM as a regulatory channel subunit.

To further investigate effects of RyR1 binding on CaM structure and Ca^{2+} sensitivity, we utilize a Ca^{2+}-sensitive fluorescent derivative of CaM that retains a high affinity for both the $RyR1_{3614-43}$ peptide and full-length RyR1. Our results suggest important differences between the effects exerted on CaM by these two types of targets.

EXPERIMENTAL PROCEDURES

Materials. Pigs were obtained from the University of Minnesota Experimental Farm. Acrylodan was purchased from Molecular Probes (Eugene, OR). Tran^{35}S-label was obtained from ICN Radiochemicals (Costa Mesa, CA). [^{3}H]-Ryanodine was purchased from NEN Life Science Products (Boston, MA). The $RyR1_{3614-43}$ 30-mer peptide derived from the proposed CaM binding site of RyR1 (*13*) was synthesized and HPLC-purified at the University of Minnesota Microchemical Facility. Other reagents were from Sigma (St. Louis, MO).

Isolation of SR Vesicles. Skeletal muscle SR vesicles were isolated from pig longissimus dorsi muscle (*16*, *17*). Briefly, muscle homogenates were subjected to differential centrifugation, and the resulting vesicles were extracted with 0.6 M KCl and subsequently fractionated on discontinuous sucrose gradients. All isolation buffers contained a mixture of protease inhibitors (100 nM aprotinin, 1 μM leupeptin, 1 μM pepstatin, 1 mM benzamidine, and 0.2 mM phenylmethanesulfonyl fluoride).

CaM Mutagenesis and Purification. Recombinant rat CaM was expressed in *Escherichia coli* using the pET-7 vector (*18*). The native threonine at position 26 ($-Y$ position of the first EF-hand Ca^{2+} binding site) was mutated to cysteine using the QuikChange mutagenesis kit (Stratagene, La Jolla, CA), and the mutation was verified by DNA sequencing. Following induction with isopropyl D-thiogalactopyranoside, WT- and T26C-CaM were purified via phenyl-Sepharose chromatography (*19*). A cysteine was also introduced at residue 26 of a Ca^{2+}-insensitive CaM mutant (CaM_{1234}), with glutamate to alanine substitutions at the $-Z$ position of each EF-hand (*20*). This mutant (termed T26C-CaM_{1234}) was subcloned into the pET-30 vector (Novagen), expressed as a His-tagged fusion protein, and purified by nickel affinity chromatography. Protein concentrations were determined by the bicinchoninic acid procedure (Pierce, Rockford, IL) using bovine brain CaM as the standard.

Labeling of CaM with Acrylodan. To eliminate potential intermolecular disulfide bridges, T26C-CaM (0.2 mM) was treated with 5 mM DTT for 2 h, in a medium containing 25 mM HEPES (pH 7.5) and 6 M GuHCl. The sample was then diluted 2-fold and subjected to phenyl-Sepharose chromatography to remove excess DTT. The concentration of CaM in the eluted samples [50 mM Tris, 0.5 mM $CaCl_2$, and 5 mM EGTA (pH 7.5)] was adjusted to 0.15 mM, and the concentration of GuHCl was adjusted to 6 M. To this sample was added acrylodan from a 100 mM stock (in DMF) to a final concentration of 1.5 mM. The sample was incubated at room temperature, protected from light, with tumbling for 4 h. The ^{ACR}CaM sample was separated from unreacted acrylodan by phenyl-Sepharose chromatography. To obtain $^{ACR}CaM_{1234}$, nickel affinity chromatography was used instead of phenyl-Sepharose chromatography. The column-immobilized His-tagged $^{ACR}CaM_{1234}$ was then treated with factor Xa protease to release the full-length labeled $^{ACR}CaM_{1234}$ with no additional N-terminal residues. The bound fluorophore was quantitated using the extinction coefficient of ^{ACR}CaM (ϵ_{bound} = 19 000 M^{-1} cm^{-1} at λ = 370 nm). The final dye:protein ratio was 0.95 $\pm$ 0.05, consistent with specific labeling of a single residue of T26C-CaM.

Matrix-Assisted Laser Desorption Ionization Time-of-Flight (MALDI-TOF) Mass Spectrometry. Specific, stoichiometric labeling of T26C-CaM with a single acrylodan moiety was confirmed by MALDI-TOF mass spectrometry carried out at the University of Minnesota Mass Spectrometry Consortium for the Life Sciences using a Bruker (Boston, MA) Biflex III mass spectrometer equipped with a N_2 laser (337 nm, pulse length of 3 ns) and a microchannel plate detector. Data were collected in the linear mode, with positive polarity, with an accelerating potential of 19 kV. External calibration was performed using trypsinogen and horse heart cytochrome *c*. The matrix used for samples and standards was a saturated solution of 3,5-dimethoxy-4-hydroxycinnamic acid in a 50:50 acetonitrile/Nanopure water mixture, with 0.1% trifluoroacetic acid. Prior to MALDI-TOF analysis, samples were desalted using C4 ZipTips (Millipore) according to the manufacturer's protocol.

Fluorescence Measurements. Fluorescence was measured in a 2 mm $\times$ 10 mm quartz cuvette. Steady-state fluorescence emission spectra were acquired using an ISS K2 fluorometer (ISS, Champaign, IL) in ratio mode, using an argon ion laser (Coherent, Santa Clara, CA) as the source of excitation at 363.8 nm. Corrected emission spectra were acquired with a step size of 1 nm, an integration time of 1 s/step, and a bandwidth of 8 nm. A matching sample blank scan was subtracted from each spectrum. The sample temperature was controlled using a recirculating water bath set to 25 °C. Ca^{2+} titrations were performed by addition of small aliquots of concentrated $CaCl_2$ to the sample in the apo buffer [20 mM K-PIPES, 120 mM K-propionate, 5 mM GSH, 0.1 mg/mL BSA, 1 μg/mL aprotinin/leupeptin, and 1.0 mM EGTA (pH 7.0)]. The free Ca^{2+} concentration was set using Ca^{2+}EGTA buffers (Bound and Determined Software) (*21*), and verified using calcium calibration buffer kits (Molecular Probes).

[^{35}S]CaM Binding. Equilibrium binding of wild-type mammalian CaM metabolically labeled with [^{35}S]methionine was assessed at 25 °C in a medium containing 0.05 mg/mL SR vesicles, 20 mM K-PIPES (pH 7.0), 150 mM K-propionate, 5 mM GSH, 1 μg/mL aprotinin/leupeptin, 0.1 mg/mL BSA, and 50 nM [^{35}S]CaM (*20*). Following 2 h incubations at room temperature, vesicles were pelleted at 80000*g* (*22*). The amount of bound [^{35}S]CaM was determined by scintillation counting after solubilization of the pellets in 2% SDS. Nonspecific binding was assessed in the presence of 10 μM unlabeled CaM. Data were normalized to maximal binding, as determined in a medium containing 500 μM Ca^{2+} and 50 nM [^{35}S]CaM.

[^{3}H]Ryanodine Binding. Ryanodine selectively binds to RyR channels in the open state; thus, [^{3}H]ryanodine binding measurements are an indicator of RyR channel activity (*23*).

Binding of [^{3}H]ryanodine to skeletal muscle SR vesicles (0.05 mg/mL) was assessed at 25 °C in a medium containing 20 mM K-PIPES (pH 7.0), 150 mM K-propionate, 5 mM GSH, 0.1 mg/mL BSA, and 7 nM [^{3}H]ryanodine. Free Ca^{2+} concentrations were set using Ca^{2+}EGTA buffers (*21*). Nonspecific binding was assessed in the presence of 20 μM nonradioactive ryanodine. All assays were performed in duplicate and were repeated using at least three different SR vesicle preparations.

Single-Channel Recording. Single-channel recordings were performed as previously described (*24*). Planar lipid bilayers were formed across a 250 μm aperture in a Delrin cup. Single-channel currents were recorded using an Axoclamp 200B patch clamp amplifier (Axon Instruments, Foster City, CA). The recording solution consisted of symmetric 100 mM KCl, 10 mM PIPES (pH 7.0), and 1 mM EGTA with the Ca^{2+} concentrations adjusted by adding small aliquots of concentrated $CaCl_2$ (*21*). Single-channel data were collected using a pulsing protocol in which the potential was held at 0 mV for 4 s between 2 s steps to −70 mV. The single-channel open probability (P_o) was calculated using FETCHAN and PSTAT (pClamp software, Axon Instruments).

RESULTS

Ca^{2+} Sensitivity of ^{ACR}CaM. Stoichiometric labeling of the T26C-CaM mutant using the acrylodan fluorophore was carried out as described in Experimental Procedures. In an initial test of ^{ACR}CaM Ca^{2+} sensitivity, we compared the Ca^{2+}-induced electrophoretic gel shifts undergone by WT-CaM, T26C-CaM, and ^{ACR}CaM. As illustrated in Figure 1A, WT-CaM exhibited a characteristic Ca^{2+}-dependent gel shift, which consisted of an increased electrophoretic mobility of CaM in the presence of a saturating Ca^{2+} concentration (*25*). We observed a similar electrophoretic mobility response to Ca^{2+} for the unlabeled T26C-CaM and for its acrylodan adduct, suggesting that mutation and chemical modification did not alter the CaM structural features responsible for the gel shift.

At 10 nM free Ca^{2+} [Figure 1B (▲)], the fluorescence spectrum of ^{ACR}CaM was broad (57 nm half-width) and structured, with a peak at 516 nm and a shoulder on its blue side, at ~486 nm. These features suggest that the probe was distributed between states of relatively high and low solvent exposure, respectively. By comparison, at 300 μM free Ca^{2+} [Figure 1B (△)], we observed a substantial decrease in the fluorescence intensity, and a red shift of the main peak from 516 to 522 nm. In addition, the spectrum at high Ca^{2+} concentrations was much narrower (45.5 nm half-width), and lacked the blue-shifted shoulder. These features suggest that binding of Ca^{2+} to ^{ACR}CaM promoted a more homogeneous fluorophore distribution, in which the level of solvent exposure of the probe was increased (*26*).

To further analyze the effects of Ca^{2+} on the ^{ACR}CaM fluorescence, we used the value of the fluorescence integral over the emission range of 440−570 nm. The dependence of the integrated ^{ACR}CaM fluorescence on the concentration of free Ca^{2+} is illustrated in Figure 1C (▲). Increasing Ca^{2+} concentrations caused a substantial decrease (>50%) in ^{ACR}CaM fluorescence with an apparent K_{Ca} of 2.7 ± 0.8 μM. For comparison, we also synthesized an acrylodan adduct of a Ca^{2+}-insensitive CaM mutant ($^{ACR}CaM_{1234}$). In contrast

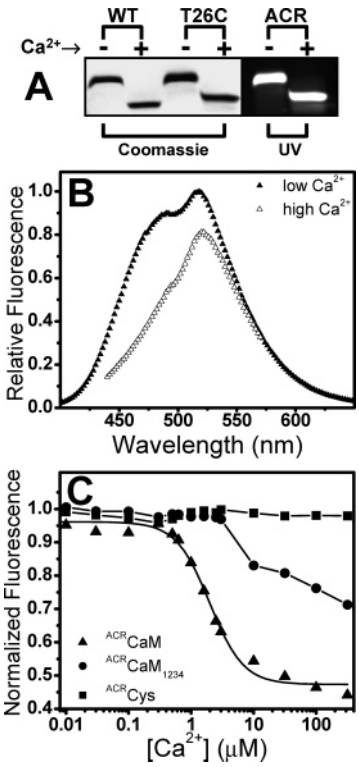

FIGURE 1: Ca^{2+} sensitivity of ^{ACR}CaM. (A) SDS−PAGE characterization of WT-CaM (WT), T26C-CaM (T26C), and ^{ACR}CaM (ACR). The arrow indicates the Ca^{2+} condition: 5 mM EGTA (−) and 5 mM $CaCl_2$ (+). Protein bands are evidenced by Coomassie dye staining (Coomassie) or by UV illumination of the gel prior to staining (UV). (B) Fluorescence spectra of ^{ACR}CaM (0.2 μM) corresponding to the low (▲) and high (△) end points of the Ca^{2+} concentration range that was scanned. Spectra are normalized to the intensity of the low-Ca^{2+} spectrum. (C) The fluorescence emission spectra of ^{ACR}CaM (▲), $^{ACR}CaM_{1234}$ (●), and acrylodan-labeled free cysteine (■) were integrated from 440 to 570 nm, and the integral values (f) were normalized (f/f_{max}) and plotted as a function of the ionized Ca^{2+} concentration. Curve represents ^{ACR}CaM fluorescence data fit to the Hill function.

to the ^{ACR}CaM probe, $^{ACR}CaM_{1234}$ was unaffected by a Ca^{2+} concentration of <10 μM [Figure 1C (●)]. At ≥10 μM Ca^{2+}, the fluorescence of $^{ACR}CaM_{1234}$ was decreased (by 25% at 100 μM), indicating that this probe bound Ca^{2+}, albeit with an affinity at least 10-fold lower than that of Ca^{2+}-sensitive ^{ACR}CaM. In addition, the fluorescence of a control consisting of the acrylodan adduct of free Cys (^{ACR}Cys) was unaffected by changes in Ca^{2+} concentration [Figure 1C (■)].

^{ACR}CaM Binding and Regulation of RyR1 Channels. To determine whether ^{ACR}CaM binds to RyR1 with an affinity similar to that of the wild-type apo- and Ca^{2+}CaM species, we examined the competitive inhibition of binding of [^{35}S]-WT-CaM to SR vesicles at nanomolar and micromolar Ca^{2+} concentrations. We observed that binding of [^{35}S]CaM to SR vesicles was fully inhibited by ^{ACR}CaM [Figure 2 (△ and ▲)] at both nanomolar (filled symbols) and micromolar Ca^{2+} concentrations (empty symbols). Furthermore, the concentration dependence of the inhibition of [^{35}S]CaM binding was similar for WT-CaM [Figure 2 (□ and ■)] and ^{ACR}CaM [Figure 2 (△ and ▲)]. Because RyR1 channels are the predominant CaM binding protein in our SR vesicle preparations (*7*, *8*, *16*), these data indicate that the affinity of ^{ACR}CaM for RyR1 channels was similar to that of the wild-type apo- and Ca^{2+}CaM species.

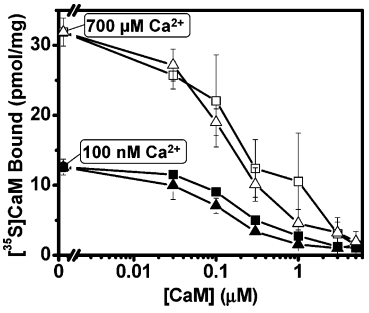

FIGURE 2: Binding of ^{ACR}CaM to skeletal muscle SR vesicles at nanomolar and micromolar Ca^{2+} concentrations. Competitive inhibition of [^{35}S]CaM binding by WT-CaM (□ and ■) or ^{ACR}CaM (△ and ▲) was assessed in media containing 0.05 mg/mL SR (~0.5 nM RyR1) and either 100 nM Ca^{2+} (filled symbols) or 700 μM Ca^{2+} (empty symbols). Data are means ± the standard error from three to five experiments.

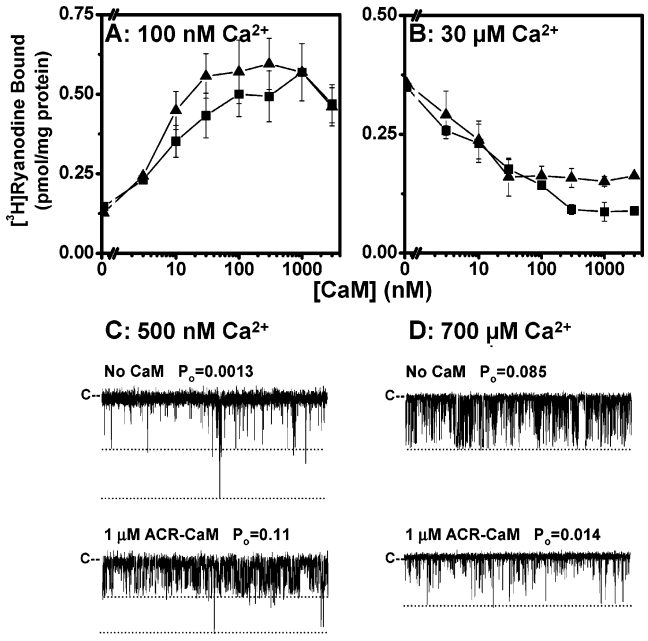

FIGURE 3: Activation and inhibition of SR vesicle [^{3}H]ryanodine binding by ^{ACR}CaM. Effects of WT-CaM (■) and ^{ACR}CaM (▲) on [^{3}H]ryanodine binding were determined in media containing 0.05 mg/mL SR and either 100 nM Ca^{2+} (A) or 30 μM Ca^{2+} (B). Data are means ± the standard error from three to six experiments. Effects of ^{ACR}CaM on RyR1 channel P_o in 500 nM Ca^{2+} (C) and 700 μM Ca^{2+} (D). Representative 1 s traces were recorded as described in Experimental Procedures. P_o values are based on a recording time of 2 min. Dashed lines represent open channel current levels. There were two channels present in the experiments whose results are shown in panel C.

To directly examine regulation of RyR1 by ^{ACR}CaM, we determined the CaM dependence of SR vesicle [^{3}H]ryanodine binding. Figure 3A shows results from experiments at nanomolar Ca^{2+} concentrations, which favors RyR1 activation by the apoCaM species. In these media, ^{ACR}CaM (3 nM to 3 μM) significantly activated [^{3}H]ryanodine binding [Figure 3A (▲)], and both the concentration dependence and the extent of activation were similar to those of WT-CaM [Figure 3A (■)]. Figure 3B shows results from experiments at micromolar Ca^{2+} concentrations, which favors inhibition of RyR1 by the Ca^{2+}CaM species. In these media, ^{ACR}CaM, like WT-CaM, significantly inhibited [^{3}H]ryanodine binding.

To further document regulation of RyR1 by ^{ACR}CaM, we examined the effects of ^{ACR}CaM on RyR1 channel P_o in lipid bilayers. In media containing sub-micromolar Ca^{2+} concentrations, RyR1 was activated by ^{ACR}CaM (Figure 3C), in accordance with the effect of WT apoCaM. Conversely, in media containing 700 μM Ca^{2+}, RyR1 P_o was reduced (Figure 3D), in accordance with the inhibitory effect of WT Ca^{2+}CaM. Together, results in Figures 2 and 3 thus indicate that both activating and inhibitory interactions of WT-CaM with RyR1 channels are retained by the ^{ACR}CaM reporter.

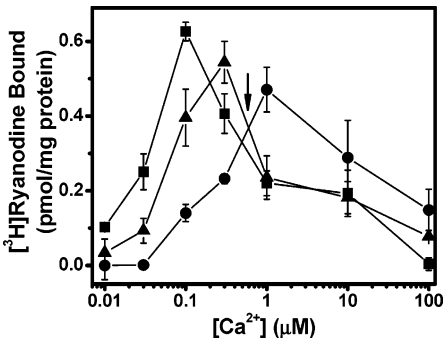

FIGURE 4: Effect of ^{ACR}CaM on the Ca^{2+} dependence of RyR1 activity. SR vesicle [^{3}H]ryanodine binding was assessed in the absence of CaM (●) or in the presence of either 2 μM WT-CaM (■) or ^{ACR}CaM (▲). The arrow indicates the crossover point at which the Ca^{2+} concentration is sufficient to promote the conversion of ^{ACR}CaM from RyR1 activator to RyR1 inhibitor. Data are means ± the standard error from four experiments.

RyR1 channel activity displays a biphasic dependence on Ca^{2+} concentration that is shifted leftward in the presence of CaM. Accordingly, Figure 4 shows that activation of RyR1 by wild-type apoCaM (<1 μM Ca^{2+}) and inhibition of RyR1 by wild-type Ca^{2+}CaM (>1 μM Ca^{2+}) resulted in a leftward shift in the Ca^{2+} dependence of SR vesicle [^{3}H]ryanodine binding. A similar leftward shift in RyR1 Ca^{2+} dependence was observed in the presence of ^{ACR}CaM. The point at which the control and the CaM curves cross may be taken to approximate the Ca^{2+} concentration at which CaM switches from the RyR1 activator (apoCaM) to inhibitor (Ca^{2+}CaM) in these steady-state experiments. Notably, for both WT-CaM and ^{ACR}CaM, the crossover point was observed between 0.3 and 1 μM Ca^{2+} (Figure 4, arrow), suggesting that WT-CaM and ^{ACR}CaM exhibit similar Ca^{2+} sensitivities when in complex with RyR1 channels.

Ca^{2+} Sensitivity of ^{ACR}CaM Fluorescence in the Presence of the RyR1 Target. To investigate the effect of the RyR1 target on the Ca^{2+} dependence of ^{ACR}CaM fluorescence, measurements were performed in the presence of 2 μM $RyR1_{3614-43}$. The interaction of ^{ACR}CaM with the soluble $RyR1_{3614-43}$ target was reflected in the ^{ACR}CaM fluorescence spectra (Figure 5A, filled symbols) both at low (10 nM) and at high (300 μM) Ca^{2+} concentrations (Figure 5A, empty symbols). At low Ca^{2+} concentrations, the effect of $RyR1_{3614-43}$ on ^{ACR}CaM fluorescence consisted mainly of an increase in the intensity of the blue-shifted shoulder. At high Ca^{2+} concentrations, the $RyR1_{3614-43}$ binding decreased the ^{ACR}CaM fluorescence intensity, but had no effect on the shape of the spectrum, which retained a single-component aspect both in the presence and in the absence of the peptide target.

To investigate interactions of ^{ACR}CaM with functional RyR1 channels in native membranes, we examined the Ca^{2+} dependence of the ^{ACR}CaM fluorescence in media containing 10 mg/mL SR (0.4 μM RyR1 CaM binding sites) (Figure 5B). In these experiments, fluorescence data acquisition was

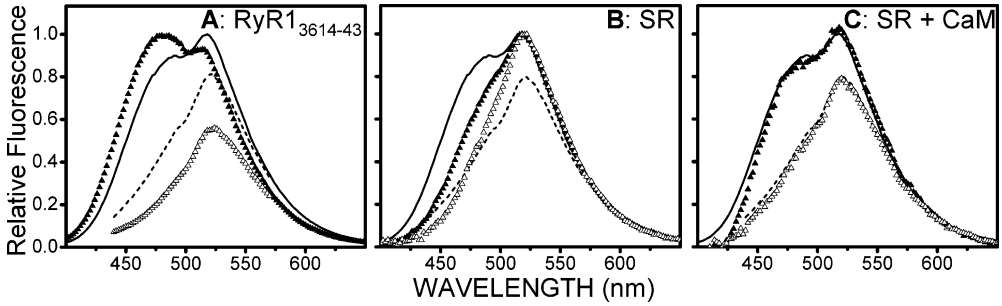

FIGURE 5: Effect of RyR1 targets on the ^{ACR}CaM fluorescence spectrum. Spectra of 0.2 μM ^{ACR}CaM in the presence of the indicated target were acquired at 10 nM Ca^{2+} (solid symbols) and 300 μM Ca^{2+} (empty symbols). (A) Spectra acquired in the presence of 2 μM $RyR1_{3614-43}$. (B) Spectra acquired in the presence of 10 mg/mL SR (0.4 μM RyR1 CaM binding sites). (C) Control spectra acquired in the presence of SR with competing, unlabeled WT-CaM (10 μM). Spectra in the absence of a target at low Ca^{2+} (solid line) and high Ca^{2+} (dashed line) concentrations are shown in each panel (replotted from Figure 1B). All spectra were corrected by subtracting corresponding blanks lacking ^{ACR}CaM and then normalized relative to the fluorescence intensity of the low-Ca^{2+} concentration spectrum.

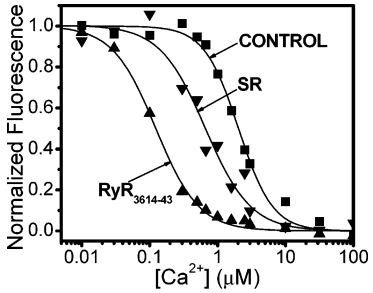

FIGURE 6: Effect of RyR1 targets on the Ca^{2+} dependence of ^{ACR}CaM fluorescence. Ca^{2+} titrations of ^{ACR}CaM (0.2 μM) were performed in the absence (■) and in the presence of either 2 μM $RyR_{3614-43}$ (▲) or 10 mg/mL SR [(▼) 0.4 μM RyR1 CaM binding sites]. Normalized plots $[(f - f_{min})/(f_{max} - f_{min})]$ of integrated ^{ACR}CaM fluorescence spectra were fit to the Hill function.

affected by intense scattering of the excitation beam, which was subtracted when ^{ACR}CaM fluorescence spectra were corrected using a baseline consisting of the SR sample without added fluorophore. This baseline was unaffected by the Ca^{2+} titration in the sample. At low Ca^{2+} concentrations in the presence of full-length, tetrameric, functional RyR1 in SR membranes, the ^{ACR}CaM fluorescence spectrum differed significantly from the spectra obtained in the absence or presence of $RyR1_{3614-43}$ (Figure 5B, filled symbols). Specifically, at low Ca^{2+} concentrations and in the presence of SR membranes, the fluorescence spectrum peaked at 518 nm; however, its blue-shifted shoulder was much less pronounced, and its half-width (47.5 ± 1.1 nm) was smaller than in the absence of SR (Figure 5B, solid line). At high Ca^{2+} concentrations, in the presence of SR, the fluorescence peak was shifted slightly to the right (to 521 nm), its height changed only negligibly relative to the low Ca^{2+} concentrations, and its half-width was slightly smaller (37.6 ± 0.4 nm) than in the presence of $RyR1_{3614-43}$. To confirm that changes in the fluorescence spectra could be attributed to the specific binding of ^{ACR}CaM to SR, fluorescence spectra were also acquired following addition of excess unlabeled WT-CaM (10 μM) (thus, blocking binding of ^{ACR}CaM to SR targets). Under these conditions, fluorescence spectra of ^{ACR}CaM were equivalent to ^{ACR}CaM spectra acquired in the absence of a target (Figure 5C).

Figure 6 summarizes the effects of RyR1 targets on the Ca^{2+} dependence of ^{ACR}CaM fluorescence. These data demonstrate that, upon incubation with the $RyR1_{3614-43}$ peptide, a pronounced leftward shift in the Ca^{2+} dependence of ^{ACR}CaM fluorescence was observed relative to controls in the absence of a target. The $RyR1_{3614-43}$ peptide caused a decrease in the apparent K_{Ca} of ^{ACR}CaM fluorescence from 2.7 ± 0.8 to 0.2 ± 0.1 μM. Remarkably, full-length RyR1 also caused a significant leftward shift in the Ca^{2+} dependence of ^{ACR}CaM fluorescence (Figure 6), but the effect was substantially smaller (apparent K_{Ca} = 0.8 ± 0.4 μM) than for $RyR1_{3614-43}$.

DISCUSSION

Defining the structure and Ca^{2+} sensitivity of CaM when in complex with RyR1 channels is key to resolving potential roles of CaM as a channel regulatory protein. Here, we use the ^{ACR}CaM adduct to investigate CaM's structure and Ca^{2+} sensitivity when in complex with RyR1 targets. We demonstrate that acrylodan labeling at CaM residue 26 yields an environment-sensitive reporter that not only retains high-affinity binding to RyR1 Ca^{2+} channels but also evokes a leftward shift in the RyR1 Ca^{2+} dependence comparable to that observed in the presence of WT-CaM. Previously, interactions of CaM with a variety of other targets have been shown to be similarly preserved following the attachment of fluorophores at this position within the N-terminal Ca^{2+} binding domain of plant CaM (*27*−*30*).

The fluorescence of ^{ACR}CaM free in solution was decreased >50% upon binding with Ca^{2+} (Figure 1C). Because acrylodan senses the polarity of its local environment (*26*), these results suggest that binding of Ca^{2+} to ^{ACR}CaM promotes movement of the acrylodan moiety to a more hydrophilic environment (*31*, *32*). This interpretation is consistent with previous evidence of a calcium-induced increase in solvent accessibility at the equivalent position of the first EF-hand of plant CaM (*31*). We further demonstrate that the Ca^{2+}-dependent decrease in fluorescence is reduced by mutations that reduce CaM's affinity for Ca^{2+} (Figure 1C). We, therefore, conclude that decreased ^{ACR}CaM fluorescence is a reflection of binding of Ca^{2+} at CaM's EF-hands. However, the extent to which this response may specifically reflect binding of Ca^{2+} at CaM's N-terminal domain or more global conformational changes resulting from Ca^{2+} binding is not yet clear.

A Ca^{2+}-dependent decrease in ^{ACR}CaM fluorescence was also observed in the presence of the $RyR1_{3614-43}$ peptide

(Figures 5A and 6); however, this effect was shifted leftward more than 10-fold relative to that in the absence of the peptide target (K_{Ca} decreased from 2.7 ± 0.8 to 0.2 ± 0.1 μM). This result is thus consistent with the previous report by Xiong and co-workers (*15*) in indicating that the $RyR1_{3614-43}$ peptide promotes a substantial increase in the Ca^{2+} affinity of CaM such that only nanomolar Ca^{2+} concentrations may be required for formation of the inhibitory Ca^{2+}CaM species. Yet, notably, extensive functional studies document that a significantly higher Ca^{2+} concentration is required for CaM's conversion to RyR1 inhibitor (Figure 4) (*8*, *12*, *20*). We therefore conclude that the structure and Ca^{2+} sensitivity of CaM when in complex with full-length channels may differ from those when in complex with the $RyR1_{3614-43}$ peptide target. Indeed, current models predict that the CaM binding pocket within full-length tetrameric RyR1 is formed by additional regions within the channel primary structure, and is therefore not likely to be fully represented by the $RyR1_{3614-43}$ peptide (*14*, *33*).

To investigate the Ca^{2+} sensitivity of CaM in complex with the full-length RyR1 channel, we determined the Ca^{2+} dependence of ^{ACR}CaM fluorescence in the presence of SR membranes. Our results indicate that the effects of full-length RyR1 on ^{ACR}CaM fluorescence are quite distinct from those of the $RyR1_{3614-43}$ peptide. Specifically, whereas the $RyR1_{3614-43}$ peptide caused an increase in the intensity of the blue-shifted shoulder at nanomolar Ca^{2+} concentrations (Figure 5*A*), this shoulder was decreased in the presence of SR (Figure 5*B*). This result suggests that upon binding to the full-length RyR1, the apoCaM probe assumes a more restricted conformation, distinct from that induced by binding to the $RyR1_{3614-43}$ peptide target. Furthermore, the magnitude of calcium's effect on the fluorescence intensity was significantly reduced in the presence of SR, suggesting that interactions with the RyR1 channels partially restricted Ca^{2+}-induced conformational transitions within ^{ACR}CaM. Nonetheless, the addition of Ca^{2+} evoked a qualitatively similar red shift of the ^{ACR}CaM spectra in the presence of SR membranes and the $RyR1_{3614-43}$ peptide, suggesting that the ^{ACR}CaM probe retains sensitivity to Ca^{2+} even when bound to full-length RyR1 channels. Alternatively, this result might be explained by the Ca^{2+} sensitivity of a small fraction of ^{ACR}CaM remaining unbound in the presence of SR. However, in opposition to this interpretation, the concentration of RyR1 CaM binding sites in our SR samples (0.4 μM) exceeds that of the ^{ACR}CaM reporter (0.2 μM), which in turn is present at a concentration >20-fold greater than the K_D of CaM−RyR1 binding (*10*, *22*). Moreover, the Ca^{2+} dependence of ^{ACR}CaM fluorescence in the presence of SR was intermediate between that in the presence of $RyR1_{3614-43}$ and that in the absence of a target (Figure 6). Finally, the Ca^{2+} dependence of the ^{ACR}CaM fluorescence in the presence of SR (K_{Ca} = 0.8 μM) is consistent with functional studies performed in equivalent media that show CaM's conversion from channel activator to channel inhibitor between 0.3 and 1 μM Ca^{2+} (Figure 4). Our results thus indicate that changes in ^{ACR}CaM fluorescence reflect binding of Ca^{2+} to the probe in complex with RyR1 channels, and that ^{ACR}CaM therefore provides a useful reporter for CaM's regulatory interactions with these channels in native SR membranes.

In conclusion, we have identified ^{ACR}CaM as a Ca^{2+}-sensitive fluorescent reporter that retains high-affinity functional interactions with RyR1 channel targets. Our results demonstrate that both the structure and Ca^{2+} sensitivity of CaM are altered upon target binding, although effects of the $RyR1_{3614-43}$ peptide and full-length channels are distinct. In the presence of full-length RyR1, our ^{ACR}CaM K_{Ca} determinations (~1 μM Ca^{2+}) fall within the physiologically relevant range of Ca^{2+} concentrations (from ~0.1 to ~10 μM), suggesting that CaM may be appropriately tuned to respond to changing Ca^{2+} concentrations in the vicinity of the channel. Additional studies defining the structure and Ca^{2+} sensitivity of CaM in complex with RyRs will help to resolve CaM's potential roles as a regulatory subunit of these channels.

ACKNOWLEDGMENT

We are grateful to Dr. Charles F. Louis for encouraging this project in its initial stages. We thank Igor Negrashov for excellent spectroscopy technical support and Octavian Cornea for assistance with the preparation of the manuscript.

REFERENCES

1. Hoeflich, K. P., and Ikura, M. (2002) Calmodulin in action: Diversity in target recognition and activation mechanisms, *Cell 108*, 739−742.
2. Vetter, S. W., and Leclerc, E. (2003) Novel aspects of calmodulin target recognition and activation, *Eur. J. Biochem. 270*, 404−414.
3. Olwin, B. B., and Storm, D. R. (1985) Calcium binding to complexes of calmodulin and calmodulin binding proteins, *Biochemistry 24*, 8081−8086.
4. Peersen, O. B., Madsen, T. S., and Falke, J. J. (1997) Intermolecular tuning of calmodulin by target peptides and proteins: Differential effects on Ca^{2+} binding and implications for kinase activation, *Protein Sci. 6*, 794−807.
5. Jurado, L. A., Chockalingam, P. S., and Jarrett, H. W. (1999) Apocalmodulin, *Physiol. Rev. 79*, 661−682.
6. Seiler, S., Wegener, A. D., Whang, D. D., Hathaway, D. R., and Jones, L. R. (1984) High molecular weight proteins in cardiac and skeletal muscle junctional sarcoplasmic reticulum vesicles bind calmodulin, are phosphorylated, and are degraded by Ca^{2+}-activated protease, *J. Biol. Chem. 259*, 8550−8557.
7. Yang, H. C., Reedy, M. M., Burke, C. L., and Strasburg, G. M. (1994) Calmodulin interaction with the skeletal muscle sarcoplasmic reticulum calcium channel protein, *Biochemistry 33*, 518−525.
8. Tripathy, A., Xu, L., Mann, G., and Meissner, G. (1995) Calmodulin activation and inhibition of skeletal muscle Ca^{2+} release channel (ryanodine receptor), *Biophys. J. 69*, 106−119.
9. Balshaw, D. M., Yamaguchi, N., and Meissner, G. (2002) Modulation of intracellular calcium-release channels by calmodulin, *J. Membr. Biol. 185*, 1−8.
10. Moore, C. P., Rodney, G., Zhang, J. Z., Santacruz-Toloza, L., Strasburg, G., and Hamilton, S. L. (1999) Apocalmodulin and Ca^{2+} calmodulin bind to the same region on the skeletal muscle Ca^{2+} release channel, *Biochemistry 38*, 8532−8537.
11. Samso, M., and Wagenknecht, T. (2002) Apocalmodulin and Ca^{2+}-calmodulin bind to neighboring locations on the ryanodine receptor, *J. Biol. Chem. 277*, 1349−1353.
12. Rodney, G. G., Williams, B. Y., Strasburg, G. M., Beckingham, K., and Hamilton, S. L. (2000) Regulation of RYR1 activity by Ca^{2+} and calmodulin, *Biochemistry 39*, 7807−7812.
13. Rodney, G. G., Moore, C. P., Williams, B. Y., Zhang, J. Z., Krol, J., Pedersen, S. E., and Hamilton, S. L. (2001) Calcium binding to calmodulin leads to an N-terminal shift in its binding site on the ryanodine receptor, *J. Biol. Chem. 276*, 2069−2074.
14. Zhang, H., Zhang, J. Z., Danila, C. I., and Hamilton, S. L. (2003) A noncontiguous, intersubunit binding site for calmodulin on the skeletal muscle Ca^{2+} release channel, *J. Biol. Chem. 278*, 8348−8355.
15. Xiong, L. W., Newman, R. A., Rodney, G. G., Thomas, O., Zhang, J. Z., Persechini, A., Shea, M. A., and Hamilton, S. L. (2002) Lobe-dependent regulation of ryanodine receptor type 1 by calmodulin, *J. Biol. Chem. 277*, 40862−40870.

16. Fruen, B. R., Bardy, J. M., Byrem, T. M., Strasburg, G. M., and Louis, C. F. (2000) Differential Ca^{2+} sensitivity of skeletal and cardiac muscle ryanodine receptors in the presence of calmodulin, *Am. J. Physiol. 279*, C724−C733.
17. Fruen, B. R., Mickelson, J. R., and Louis, C. F. (1997) Dantrolene inhibition of sarcoplasmic reticulum Ca^{2+} release by direct and specific action at skeletal muscle ryanodine receptors, *J. Biol. Chem. 272*, 26965−26971.
18. Wang, S., George, S. E., Davis, J. P., and Johnson, J. D. (1998) Structural determinants of Ca^{2+} exchange and affinity in the C terminal of cardiac troponin C, *Biochemistry 37*, 14539−14544.
19. Gopalakrishna, R., and Anderson, W. B. (1982) Ca^{2+}-induced hydrophobic site on calmodulin: Application for purification of calmodulin by phenyl-Sepharose affinity chromatography, *Biochem. Biophys. Res. Commun. 104*, 830−836.
20. Fruen, B. R., Black, D. J., Bloomquist, R. A., Bardy, J. M., Johnson, J. D., Louis, C. F., and Balog, E. M. (2003) Regulation of the RYR1 and RYR2 Ca^{2+} release channel isoforms by Ca^{2+}-insensitive mutants of calmodulin, *Biochemistry 42*, 2740−2747.
21. Brooks, S. P., and Storey, K. B. (1992) Bound and Determined: A computer program for making buffers of defined ion concentrations, *Anal. Biochem. 201*, 119−126.
22. Balshaw, D. M., Xu, L., Yamaguchi, N., Pasek, D. A., and Meissner, G. (2001) Calmodulin binding and inhibition of cardiac muscle calcium release channel (ryanodine receptor), *J. Biol. Chem. 276*, 20144−20153.
23. Tanna, B., Welch, W., Ruest, L., Sutko, J. L., and Williams, A. J. (1998) Interactions of a reversible ryanoid (21-amino-9α-hydroxyryanodine) with single sheep cardiac ryanodine receptor channels, *J. Gen. Physiol. 112*, 55−69.
24. Balog, E. M., Fruen, B. R., Kane, P. K., and Louis, C. F. (2000) Mechanisms of P_i regulation of the skeletal muscle SR Ca^{2+} release channel, *Am. J. Physiol. 278*, C601−C611.
25. Maune, J. F., Klee, C. B., and Beckingham, K. (1992) Ca^{2+} binding and conformational change in two series of point mutations to the individual Ca^{2+}-binding sites of calmodulin, *J. Biol. Chem. 267*, 5286−5295.
26. Prendergast, F. G., Meyer, M., Carlson, G. L., Iida, S., and Potter, J. D. (1983) Synthesis, spectral properties, and use of 6-acryloyl-2-dimethylaminonaphthalene (Acrylodan). A thiol-selective, polarity-sensitive fluorescent probe, *J. Biol. Chem. 258*, 7541−7544.
27. Zot, H. G., Aden, R., Samy, S., and Puett, D. (1990) Fluorescent adducts of wheat calmodulin implicate the amino-terminal region in the activation of skeletal muscle myosin light chain kinase, *J. Biol. Chem. 265*, 14796−14801.
28. Strasburg, G. M., Hogan, M., Birmachu, W., Thomas, D. D., and Louis, C. F. (1988) Site-specific derivatives of wheat germ calmodulin. Interactions with troponin and sarcoplasmic reticulum, *J. Biol. Chem. 263*, 542−548.
29. Gao, J., Yao, Y., and Squier, T. C. (2001) Oxidatively modified calmodulin binds to the plasma membrane Ca-ATPase in a nonproductive and conformationally disordered complex, *Biophys. J. 80*, 1791−1801.
30. Mills, J. S., Walsh, M. P., Nemcek, K., and Johnson, J. D. (1988) Biologically active fluorescent derivatives of spinach calmodulin that report calmodulin target protein binding, *Biochemistry 27*, 991−996.
31. Yao, Y., Schoneich, C., and Squier, T. C. (1994) Resolution of structural changes associated with calcium activation of calmodulin using frequency domain fluorescence spectroscopy, *Biochemistry 33*, 7797−7810.
32. Watkins, A. N., and Bright, F. V. (1998) Effects of Fluorescent Reporter Group Structure on the Dynamics Surrounding Cysteine-26 in Spinach Calmodulin: A Model Biorecognition Element, *Appl. Spectrosc. 52*, 1447−1456.
33. Yamaguchi, N., Xin, C., and Meissner, G. (2001) Identification of apocalmodulin and Ca^{2+}-calmodulin regulatory domain in skeletal muscle Ca^{2+} release channel, ryanodine receptor, *J. Biol. Chem. 276*, 22579−22585.

BI048246U